JOURNAL OF CATALYSIS **138,** 206–222 (1992)

# Mechanism of Formation Oxygenated Compounds from CO + $H_2$ Reaction over $SiO_2$-Supported Ru–Co Bimetallic Carbonyl Cluster-Derived Catalysts

FENG-SHOU XIAO,*,†,[1] ATSUSHI FUKUOKA,* AND MASARU ICHIKAWA*

*Catalysis Research Center, Hokkaido University, Sapporo 060, Japan; and †Department of Chemistry, Jilin University, Changchun 130023, China

Received December 17, 1991; revised March 6,1992

The catalytic performance in CO hydrogenation over Ru, Ru–Co, and Co carbonyl cluster-derived catalysts has been investigated, and it was found that the activity and selectivity for oxygenated products on a series of Ru–Co/$SiO_2$ catalysts are much higher than those on $Ru_3/SiO_2$ and $Co_4/SiO_2$ catalysts. The mechanism of oxygenated formation on these Ru–Co/$SiO_2$ catalysts has been investigated by *in situ* infrared, mass, and X-ray photoelectron spectroscopies. The IR spectra of reaction of CO + $H_2$ with Ru–Co/$SiO_2$ catalysts show a band appearing at 1584 $cm^{-1}$, which has a good relationship to the activity and selectivity for oxygenates in CO hydrogenation. The adsorption of CO on reduced Ru–Co/$SiO_2$ catalysts prepared from Ru–Co bimetallic carbonyl clusters exhibits a band at 1680 $cm^{-1}$ shifting to 1640 $cm^{-1}$ with $^{13}CO$, which is assigned to the C- and O-ended CO chemisorbed on Ru–Co/$SiO_2$ catalysts. The chemical trapping of 1584 $cm^{-1}$ adspecies shows that the 1584 $cm^{-1}$ species reacts with $H_2$ to produce $CH_4$ and $CH_3OH$, and the addition of $D_2$ to 1584 $cm^{-1}$ species results in the formation of $CHD_3$ and $CHD_2OD$. With the increase of reaction time and temperature, we find the bands at 1555 and 1440–1470 $cm^{-1}$, while the 1584 $cm^{-1}$ band gradually decreases on Ru–Co/$SiO_2$ catalysts. XPS spectra demonstrate that the Ru and Co sites on the surface of Ru–Co/$SiO_2$ catalysts are in the chemical state of $Ru^0$ and $Co^{2+}$, respectively, and it is suggested that the bimetallic $Ru^0$–$Co^{2+}$ sites are very active centers for the formation of oxygenates in CO hydrogenation. Considering the product distribution at various reaction temperatures, it is suggested that the 1584 and 1555 $cm^{-1}$ species possibly assigned to formyl and acyl are precursors to methanol and higher $C_2$-oxygenates, respectively, and the 1584 $cm^{-1}$ species can be converted into 1555 $cm^{-1}$ species by reaction with an alkyl group. © 1992 Academic Press, Inc.

## INTRODUCTION

The chemical modification of solid surfaces, e.g., MgO, $SiO_2$, and $SiO_2$–$Al_2O_3$ and zeolites by using organometallic carbonyl clusters as precursors has been a subject of recent interest (*1–3, 5*). The supported clusters provide highly dispersed metal particles in a uniform size distribution, with a discrete metal composition of the precursor bimetallic clusters. These catalysts exhibit good catalytic performance in CO hydrogenation and offer higher activities and selectivities, compared with the conventional catalysts prepared by coimpregnation and ion exchange of metal salts (*1–4*). It has been previously reported that the CO hydrogenation over transition metal catalysts produces a variety of compounds such as hydrocarbons, alcohols, aldehydes, and acids, and some electropositive ions such as Mn, Ti, Zr, Nb, and Fe promote the production of oxygenates such as aldehydes and alcohols in CO hydrogenation catalyzed on Rh and Pd (*6–8*). As a localized model for the promotion of Rh and Pd, tailored metal catalysts have been prepared from $SiO_2$-supported Rh–Fe (*9–10*) and Pd–Fe (*11*) bime-

---

[1] Permanent address: Department of Chemistry, Jilin University, Changchun 130023, China. To whom correspondence should be addressed.

0021-9517/92 $5.00

tallic carbonyl clusters, and it has been demonstrated that they provide higher activities and improved selectivities for $C_1$ and $C_2$ alcohols from CO + $H_2$ reaction compared with those from the homometallic cluster-derived catalyst and even those of the conventional bimetallic catalysts.

On the other hand, the mechanism of hydrocarbon and oxygenate formation in CO hydrogenation has been widely investigated in the past decades (*12–22*). These results strongly suggest that the surface carbon formed by the dissociation of CO is an intermediate for hydrocarbon formation (*12–16*) and that the formation of oxygenates involves the insertion of CO into adsorbed species such as methyl and carbene (*17–22*). Notably, several intermediates for forming oxygenates have been proposed, such as formate (*23–29*), carbonate (*18*), acetyl (*19, 20*), and acetate (*17, 19, 20*).

In the present study, we prepared a series of Ru–Co bimetallic catalysts using $SiO_2$ impregnated with a series of Ru–Co bimetallic carbonyl clusters, and we studied the activity and selectivity in CO hydrogenation (*30–34*). The mechanism of formation of oxygenates from CO hydrogenation has been studied through reaction kinetics, infrared spectra of adsorbed species, isotopic tracers, and X-ray photoelectron spectroscopy. It is found that two adspecies having IR bands at 1584 and 1555 $cm^{-1}$ are very active in producing methanol and higher $C_2$-oxygenates, respectively.

## EXPERIMENTAL

### *Materials and Catalyst Preparation*

Various gases such as $H_2$, CO, $O_2$, $N_2$, and CO + $H_2$, with purities >99.999%, were supplied by Takachiho Trading Co. Isotopic labeled gases of $^{13}CO$ (purity 99.3%) and $D_2$ (purity 99.9%) were purchased from MSD Isotopes. The aldehydes and alcohols were purified by outgassing and vacuum distillation from a dry ice–methanol cold trap to a liquid nitrogen cold trap.

All manipulations were performed in an inert atmosphere by the use of a glove box for catalyst preparation. Clusters such as $[Et_4N][HRu_3(CO)_{11}]$, $H_3Ru_3Co(CO)_{12}$, $RuCo_2(CO)_{11}$, $HRuCo_3(CO)_{12}$, and $Ru_3Co_3C(CO)_{14}$ were synthesized according to the literature (*35–38*). Each cluster-derived catalyst was prepared by impregnation of $SiO_2$ (Davison GR-10303, surface area 330 $m^2/g$) with a solution of cluster in dry acetone. Each catalyst contained about 3 wt% Ru for IR characterization and 1 wt% Ru for CO hydrogenation and with Ru content controlled by use of the appropriate amount of the cluster in the slurry. Prior to use, the $SiO_2$ was pretreated in flowing oxygen at 573 K overnight and then evacuated at 573 K for 2 h. In a typical run, 240 mg (or 80 mg) of $H_3Ru_3Co(CO)_{12}$ in 100 ml of acetone was brought in contact with 3.3 g of $SiO_2$. After being stirred for 2 h the solvent was evaporated from the slurry under vacuum. The solid was oxidized in $O_2$ flow ($1 \times 10^5$ Pa, 40 ml/min) at 423 K for 2 h in a glass tube, followed by reduction in a $H_2$ flow ($1 \times 10^5$ Pa, 40 ml/min) at the programmed temperatures 293 to 573 K and 573 K for 2 h.

### *CO Hydrogenation*

The CO hydrogenation reaction was carried out at 423–523 K with a continuous-flow stainless-steel microreactor, where 1 g of the catalyst (Ru loading 1 wt%) was charged. A gas mixture of CO and $H_2$ ($CO/H_2 = 1/2$, $5 \times 10^5$ Pa) was introduced into the reactor at a flow rate of 40 ml/min and a space velocity of 444 $h^{-1}$. Oxygenated products were collected in a water trap (50 ml of $H_2O$) by bubbling the effluent gas through it and analyzed by GC-8AIF gas chromatography with a flame ionization detector. CO, $CO_2$, and hydrocarbons were separated by using Shimadzu GC-8AIF gas chromatography with a thermal conductivity detector. In gas chromatography, concentrations of the products were calculated with an intergator (Shimadzu Chromatopac CR-3A).

### *Infrared Spectroscopy (IR)*

Each catalyst (Ru loading 3 wt%) was pressed into a self-supporting disk (15 mm

TABLE 1

CO Hydrogenation on $SiO_2$-Supported Ru, Ru–Co, and Co Carbonyl Cluster-Derived Catalysts[a]

| Precursor | TOF (mmol/mol(Ru)min) | | | | | Selectivity (%) | | |
|---|---|---|---|---|---|---|---|---|
| | Co/Ru | CO(%) | Hydrocar. | Oxy. | $CO_2$ | Oxy.[b] | MeOH[c] | Higher oxy.[d] |
| $[HRu_3(CO)_{11}]^-$ | – | 0.32 | 21 | 0.2 | — | 1.0 | 30 | 70 |
| $H_3Ru_3Co(CO)_{12}$ | 0.33 | 2.5 | 130 | 18 | 6.7 | 12 | 18 | 82 |
| $RuCo_2(CO)_{11}$ | 2.0 | 4.4 | 220 | 32 | 9.4 | 12 | 15 | 85 |
| $HRuCo_3(CO)_{12}$ | 3.0 | 9.8 | 525 | 55 | 33 | 9.0 | 21 | 79 |
| $RuCl_3 + CoCl_2$ | 3.0 | 2.2 | 124 | 3.4 | 4.7 | 2.6 | 20 | 80 |
| $Co_4(CO)_{12}$[e] | — | 0.12 | 6.0 | 1.2 | — | 17 | 41 | 59 |
| $[HRu_3(CO)_{11}]^- + Co_4(CO)_{12}$ | 3.0 | 1.0 | 53 | 2.8 | 3.0 | 4.8 | 19 | 81 |

[a] $CO/H_2 = 0.5$; flow rate 40 ml/min; total pressure $5 \times 10^5$ Pa.

[b] Molar ratio of $\Sigma iC_i$ ($i$ = 1–5, oxygenates)/[$\Sigma iC_i$($i$ = 1–5, oxygenates) + $\Sigma iC_i$ ($i$ = 1–5, hydrocarbons)].

[c] Molar ratio of MeOH/$\Sigma iC_i$ ($i$ = 1–5, oxygenates).

[d] Molar ratio of $\Sigma iC_i$ ($i$ = 2–5, oxygenates)/$\Sigma iC_i$ ($i$ = 1–5, oxygenates).

[e] Rate of formation (mmol/mol(co)min).

in diameter and 10–12 mg/cm$^2$ in weight) and the catalyst disk was placed in an infrared quartz cell with $CaF_2$ windows. After reduction for 2 h at 573 K in $H_2$ flow (40 ml/min), the sample disk was cooled to room temperature. Then, reaction gases (40 ml/min, $1 \times 10^5$, $CO/H_2 = 1/2$) were introduced into the cell, and infrared spectra were measured by using a Fourier transform spectrometer (FT-IR 4100, Shimadzu Co.) with a resolution of 2 cm$^{-1}$ in the region 4000–1000 cm$^{-1}$.

### *Mass Spectroscopy (MS)*

When the working vacuum of the mass spectrometer reached $10^{-1}$–$10^{-2}$ Pa, the gas phase was continuously monitored by the mass spectrometer (AQ-200, Anelva Co.) under various reaction conditions.

### *X-ray Photoelectron Spectroscopy (XPS)*

Catalysts (Ru loading 3 wt%) were pressed into self-supporting disks (15 mm in diameter and 30 mg/cm$^2$ in weight) and placed into the stainless-steel chamber with an upper high vacuum ($10^{-6}$ Pa). The Ru $3d$ and Co $3p$ spectra were measured with V. G. ESCALAB Mark II system. An AlK$\alpha$ X-ray source ($h\nu$ = 1486.6 ev) was used, and the X ray was operated at 14 kV and 20 mA. The binding energies were calculated by taking the energy of the $2p$ of silicon atom (104.0 eV) as an internal standard.

## RESULTS

### *Reaction Kinetics and Product Distribution*

The catalytic properties of the various Ru–Co bimetallic catalysts prepared from Ru–Co bimetallic carbonyl clusters in the $CO + H_2$ reaction at 519 K were investigated, and the results are presented in Table 1. The activity and selectivity for product on various catalysts show a large difference depending on the precursors of Ru–Co bimetallic carbonyl clusters. The $Ru_3/SiO_2$ catalyst prepared from $[HRu_3(CO)_{11}]^-$ has low activity (0.32%) for CO conversion and almost does not form oxygenates. $Co_4/SiO_2$ prepared from a $Co_4(CO)_{12}$ cluster exhibits a much lower conversion (0.12%), but the selectivity for oxygenates is 16%. On the Ru–Co bimetallic catalysts prepared from $H_3Ru_3Co(CO)_{12}$, $RuCo_2(CO)_{11}$, and $HRuCo_3(CO)_{12}$ clusters, the CO conversion and the rates for oxygenates are substantially

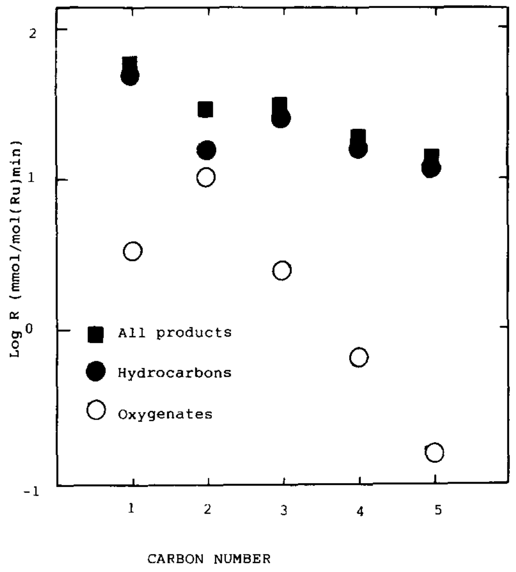

FIG. 1. Typical product distribution of CO hydrogenation in an Anderson–Schulz–Flory plot on $Ru_3Co/SiO_2$ prepared from $H_3Ru_3Co(CO)_{12}$ bimetallic carbonyl cluster.

increased. Notably, with an increase in the molar ratio Co/Ru in Ru–Co bimetallic clusters, the activity and selectivity for hydrocarbons and oxygenates are highly increased. The above results indicate that atomic Co in Ru–Co bimetallic cluster-derived catalysts remarkably promotes the formation of oxygenates.

To determine the effect of proximity of Ru and Co in the precursor compounds, two Ru–Co catalysts were prepared from $RuCl_3$ + $CoCl_2$ and from a mixture of monometallic clusters $[HRu_3(CO)_{11}]^-$ and $Co_4(CO)_{12}$ at the same Co/Ru molar ratio of 3.0 as that of $HRuCo_3(CO)_{12}$ showing the most activity in total Ru–Co bimetallic cluster-derived catalysts. Both catalysts give larger rates for hydrocarbons and oxygenates than that on $Ru_3/SiO_2$ and $Co_4(CO)_{12}$, but relative enhancement of the rates is much lower than that on Ru $Co_3/SiO_2$.

Figure 1 shows a typical hydrocarbon distribution of the CO + $H_2$ reaction in an Anderson–Schulz–Flory plot on the $Ru_3Co/SiO_2$ catalyst. The hydrocarbon distribution obeys the ASF plots apart from $C_2$, and the rates of oxygenated formation are in good agreement with ASF equation from $C_2$ to $C_5$. All products in CO + $H_2$ reaction basically follow the ASF plots.

Table 2 presents the temperature dependency of the $Ru_3Co/SiO_2$ catalyst. An obvious feature is that hydrocarbon formation quickly decreases with the temperature and at low temperature the oxygenates mainly consist of methanol. Although the selectivity for oxygenates in the products decreases considerably with increasing reaction temperature, the selectivity for higher $C_2$-oxy-

TABLE 2

Catalytic Performance on Ru–Co Catalyst Prepared from $HRuCo_3(CO)_{12}$ Carbonyl Cluster in CO Hydrogenation at Various Temperatures[a]

| Temp. (K) | CO (%) | TOF (mmol/mol(Ru)min) | | | Selectivity (%) | |
|---|---|---|---|---|---|---|
| | | Hydrocar. | Oxy. | $CO_2$ | Oxy.[b] | Higher oxy.[c] |
| 458 | 1.3 | 59 | 25 | 1.0 | 30 | 59 |
| 498 | 4.7 | 234 | 40 | 8.5 | 16 | 70 |
| 519 | 9.8 | 516 | 53 | 33 | 8.9 | 77 |
| 541 | 20 | 1110 | 64 | 123 | 5.1 | 85 |

[a] $CO/H_2 = 0.5$; flow rate 40 ml/min; total pressure $5 \times 10^5$ Pa.

[b] Molar ratio of $\Sigma iC_i$ ($i$ = 1–5, oxygenates)/[$\Sigma iC^i$ ($i$ = 1–5, hydrocarbons) + $\Sigma iC_i$ ($i$ = 1–5, oxygenates)].

[c] Molar ratio of $\Sigma iC_i$ ($i$ = 2–5, oxygenates)/$\Sigma iC_i$ ($i$ = 1–5, oxygenates).

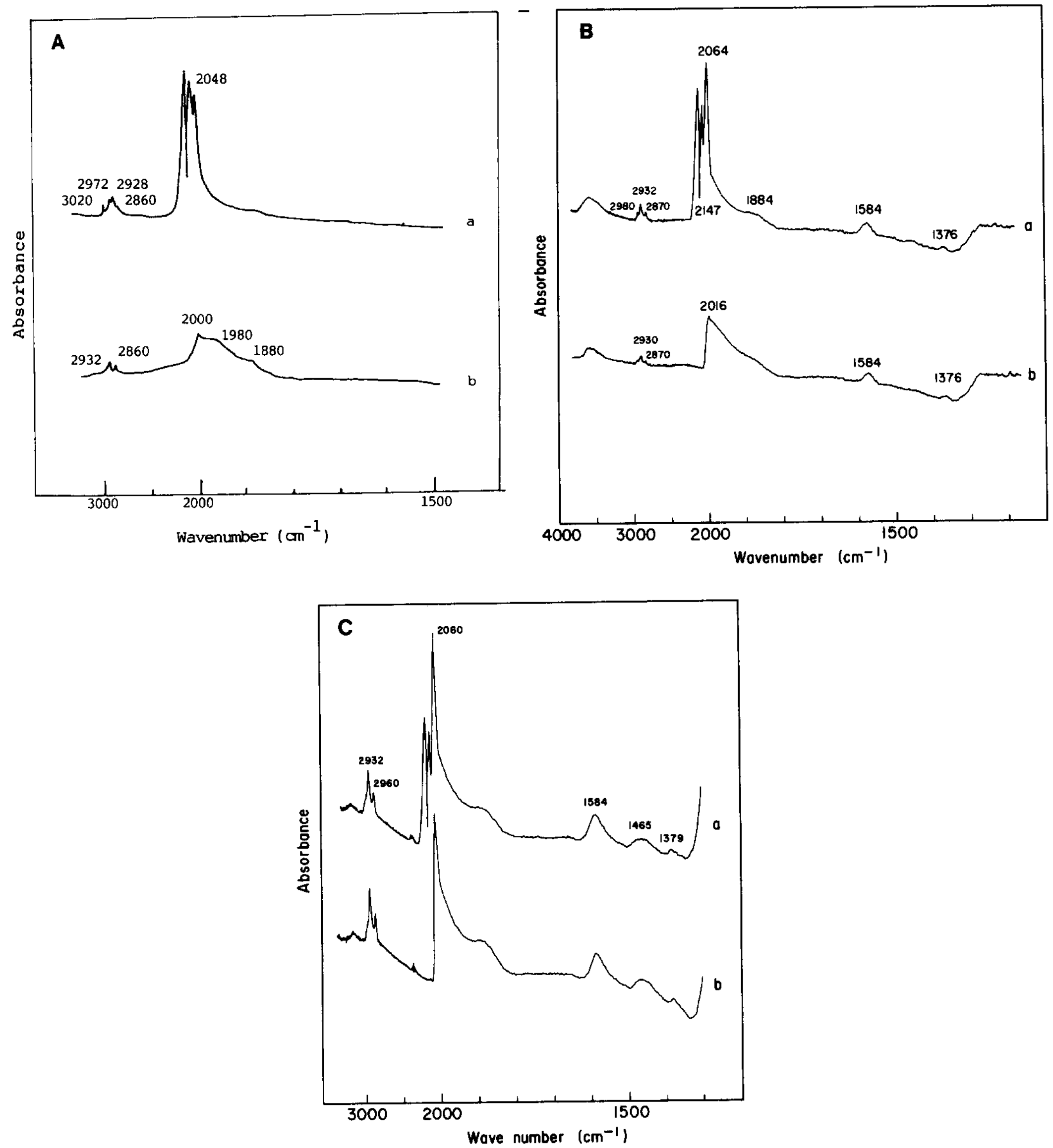

FIG. 2. IR spectra of the catalyst after reaction with CO + $H_2$. (A) $[HRu_3(CO)_{11}]^-$, (B) $H_3Ru_3Co(CO)_{12}$, (C) $HRuCo_3(CO)_{12}$ carbonyl cluster-derived catalyst reduced for 4 h at 573 K. (a) The reaction of syngas for 14 h at 453 K; (b) after a, evacuation for 20 min at room temperature.

genates increases with the temperature. This indicates that the higher $C_2$-oxygenates are predominant in the oxygenates at higher temperature.

### *IR Spectra of CO + $H_2$ on Catalyst*

Figure 2 shows the *in situ* IR spectra of the CO + $H_2$ reaction with various catalysts in CO hydrogenation at 453 K. Reaction of CO + $H_2$ for 10 h at 453 K over $Ru_3/SiO_2$ catalyst prepared from $[HRu_3(CO)_{11}]^-$ gives a broad band around 2048 cm$^{-1}$, with weak bands at 3020–2860 cm$^{-1}$. After evacuation for 20 min at 293 K to remove the gas phase, the sample spectrum exhibits broad bands at 2000, 1980, and 1880 cm$^{-1}$ and two weak

TABLE 3

The Intensities (Absorbance) of Infrared Bands at 2050, 1880, and 1584 cm$^{-1}$ and Rates of Product Formation in CO Hydrogenation on Ru, Ru–Co Catalyst Prepared from Ru, and Ru–Co Carbonyl Clusters

| Precursor | Band intensity[a] | | | TOF of oxygenates (mmol/mol(Ru)min)[b] |
|---|---|---|---|---|
| | 2050 | 1880 | 1584 | |
| $[HRu_3(CO)_{11}]^-$ | 0.24 | 0.018 | 0 | 0.79 |
| $H_3Ru_3Co(CO)_{12}$ | 0.31 | 0.038 | 0.035 | 9.1 |
| $RuCo_2(CO)_{11}$ | 0.33 | 0.045 | 0.058 | 12.8 |
| $HRuCo_3(CO)_{12}$ | 0.49 | 0.079 | 0.13 | 34.6 |

[a] CO/H$_2$ = 0.5; 1 kg/cm$^2$; reaction for 10 h; 453 K.
[b] CO/H$_2$ = 0.5, 5 × 10$^5$ Pa; 498 K.

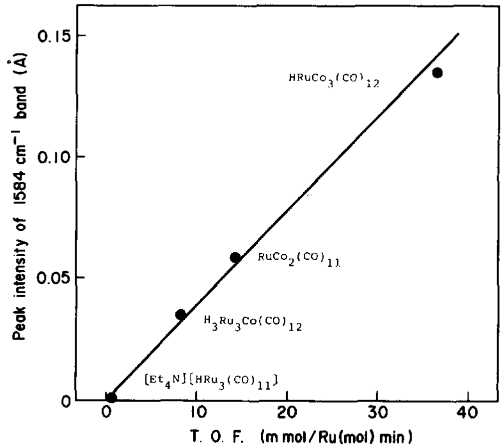

FIG. 3. A curve of the rate of formation for oxygenates in CO hydrogenation versus 1584 cm$^{-1}$ band intensity on various Ru–Co carbonyl cluster-derived catalysts.

bands at 2932 and 2860 cm$^{-1}$. The broad bands at 2000–1980 and 1880 cm$^{-1}$ are assigned to linear and bridging CO on the Ru surface (*39, 5*), respectively, and 2930 and 2860 cm$^{-1}$ are due to the C–H stretching frequencies (*40*). On the other hand, for the Ru–Co catalysts, it is very interesting to note that in addition to the bands at 2930, 2860, 2060, and 1880 cm$^{-1}$, new bands at 1584 and 1377 cm$^{-1}$ are observed. Table 3 summarizes the intensity of these IR bands and the rate of oxygenated formation on various Ru–Co bimetallic catalysts. A good linear relationship is observed between the 1584 cm$^{-1}$ band intensity and the rate of oxygenate formation, which indicates that the 1584 cm$^{-1}$ species plays an important role in production of oxygenates, as shown in Fig. 3.

It has been seen that the selectivity for oxygenates is influenced by CO conversion. At a similar CO conversion, the selectivity for oxygenates and the 1584 cm$^{-1}$ band intensity on various Ru–Co bimetallic carbonyl cluster-derived catalysts are listed in Table 4. The selectivity for oxygenates increases with an increase in the 1584 cm$^{-1}$ intensity, which further illustrates that the species responsible for the 1584 cm$^{-1}$ is a precursor to oxygenates.

The change in the CO/H$_2$ molar ratio from 0.5 to 1.0 leads to an increase of selectivity for oxygenates on Ru–Co bimetallic carbonyl-derived catalysts (*41*). Similarly, FT–IR studies reveal that the 1584 cm$^{-1}$ band intensity increases extensively with the change of CO/H$_2$ ratio. Plots of 1584 cm$^{-1}$ intensity and selectivity for oxygenates versus CO/H$_2$ offer two curves, as shown in Fig. 4. We observe that the selectivity for oxygenates linearly increases with 1584 cm$^{-1}$ band intensity.

### *Isotopic Effect of $^{13}$C- and D-Labeled CO and H$_2$*

As shown in Fig. 5, the reaction of

TABLE 4

The Selectivity for Oxygenates in CO Hydrogenation and 1584 cm$^{-1}$ Band Intensity (Absorbance) in IR Spectra on Various Ru–Co Bimetallic Carbonyl Cluster-Derived Catalysts

| Precursors | Conv.[a] of CO | React. temp. (K) | Sel. (%)[b] for oxygenates | Intensity (A)[c] of 1584 cm$^{-1}$ |
|---|---|---|---|---|
| $[HRu_3(CO)_{11}]^-$ | 0.82 | 540 | 4.1 | 0 |
| $H_3Ru_3Co(CO)_{12}$ | 0.71 | 498 | 18 | 0.035 |
| $RuCo_2(CO)_{11}$ | 0.91 | 498 | 26 | 0.058 |
| $HRuCo_3(CO)_{12}$ | 1.3 | 458 | 30 | 0.13 |

[a] Molar ratio of product and reactant based on CO.
[b] Molar ratio of $\Sigma iC_i$ ($i$ = 1–5, oxygenates)/[$\Sigma iC_i$ ($i$ = 1–5, oxygenates) + $\Sigma iC_i$ ($i$ = 1–5, hydrocarbons)].
[c] Intensity of adspecies on Ru–Co bimetallic carbonyl cluster-derived catalysts formed by reaction of syngas for 10 h at 453 K.

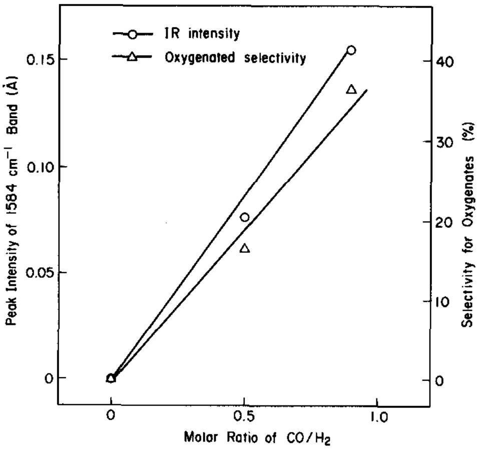

FIG. 4. Plots of 1584 $cm^{-1}$ intensity and selectivity for oxygenates versus molar ratio of $CO/H_2$ in CO hydrogenation on $HRuCo_3(CO)_{12}$ carbonyl cluster-derived catalyst.

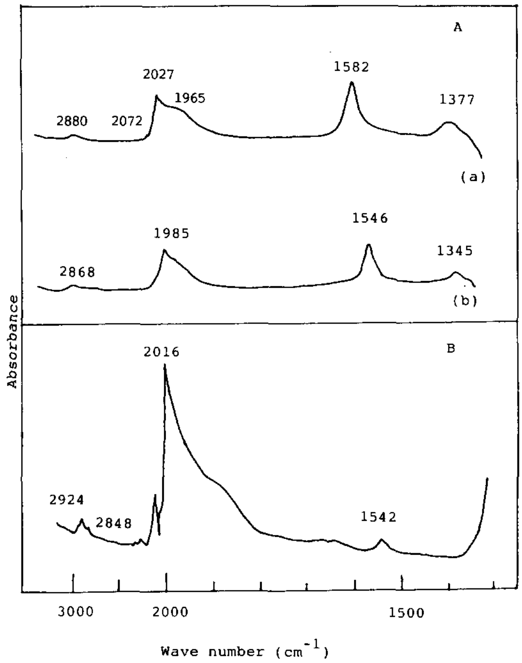

FIG. 5. (A) (a) IR spectra of the reduced $Ru_3Co_3C(CO)_{14}$ carbonyl cluster-derived catalyst (reduction for 2 h at 573 K) after reaction with 100 Torr of $^{13}CO$ and 200 Torr of $H_2$ for 4 h at 453 K, and (b) after a, evacuation at 453 K for 20 min. (B) IR spectra of the reduced $HRuCo_3(CO)_{12}$ carbonyl cluster-derived catalyst (reduction for 2 h at 573 K) after reaction with 100 Torr of $^{13}CO$ and 200 Torr of hydrogen for 2 h at 453 K.

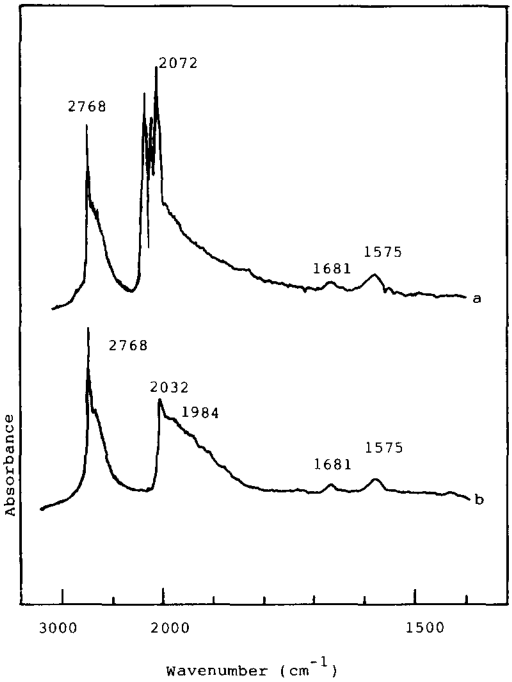

FIG. 6. IR spectra of the reduced $Ru_3Co_3C(CO)_{14}$ carbonyl cluster-derived catalyst (reduction at 2 h at 573 K) after reaction with CO + $D_2$. (a) The reaction of CO + $D_2$ for 1 h at 443 K; (b) after a, the evacuation for 20 min at 443 K.

$^{13}CO + H_2$ on $RuCo_3/SiO_2$ and $Ru_3Co/SiO_2$ gives the bands shifted to low wave numbers due to isotopic effects (Fig. 5), suggesting that the 1584 and 1377 $cm^{-1}$ bands in Fig. 2 are closely related to the CO group, in comparison with the reaction of $CO + H_2$.

The spectrum of $D_2$ + CO on $Ru_3Co_3/SiO_2$ provides the bands at 2768, 2032, 1884, 1681, and 1575 $cm^{-1}$, as shown in Fig. 6. The band at 2768 $cm^{-1}$ is assigned to the stretching frequency of hydroxyl (O–D) groups on the $SiO_2$ surface due to the H–D exchange reaction, and 2032 and 1884 $cm^{-1}$ are attributed to linear and bridging CO adsorption. The 1575 $cm^{-1}$ is reasonably assigned to shifting from the 1584 $cm^{-1}$ species in Fig. 2, which indicates that the 1584 $cm^{-1}$ species also contains the H atom. In general, $D_2$ instead of $H_2$ would result in a large difference in infrared frequency if the 1584 $cm^{-1}$ band were assigned to the C–H

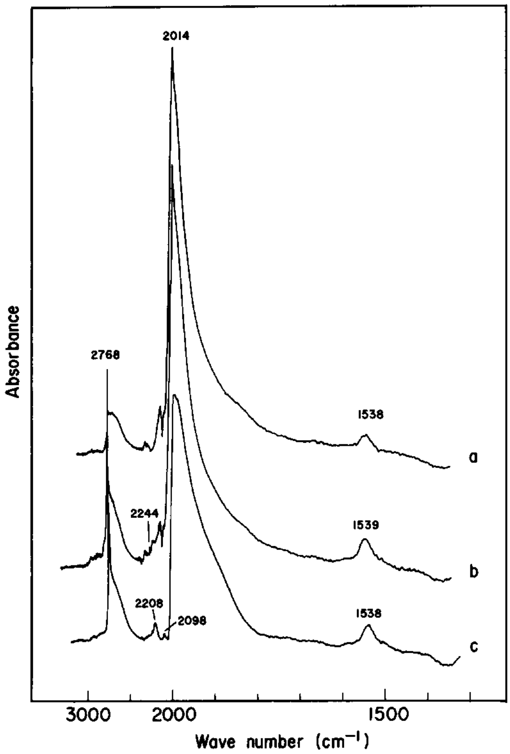

FIG. 7. IR spectra of the $^{13}CO + D_2$ reaction with reduced $HRuCo_3(CO)_{12}$ carbonyl cluster-derived catalyst (reduction at 573 K for 4 h). (a) The $^{13}CO + D_2$ reaction for 30 min at 453 K; (b) the reaction for 15 h at 453 K; (c) after b, evacuation for 20 min at room temperature.

stretching frequency (*42*). However, in our case there is a small difference between 1584 and 1575 cm$^{-1}$ under CO + $H_2$ and CO + $D_2$, respectively. Therefore, we suggest that the 1584 cm$^{-1}$ species could not be assigned to the C–H bond.

Exposure of $RuCo_3/SiO_2$ to $^{13}CO + D_2$ adds new features to IR spectra, which exhibit a further shift for the 1584 cm$^{-1}$ species due to isotopic effect of both $^{13}C$ and D, appearing at 1539 cm$^{-1}$, as shown in Fig. 7. This demonstrates that the 1584 cm$^{-1}$ species consists of both H and CO groups.

### *Adsorption of CO on Ru–Co/SiO$_2$ Catalysts*

As shown in Fig. 8, upon CO admission at 300–344 K onto the freshly reduced $Ru_3Co_3C(CO)_{14}$ and $HRuCo_3(CO)_{12}$ the two adsorption bands at 2072 and 2036 cm$^{-1}$ and 1960 cm$^{-1}$ on Ru are observed. Moreover, a low-frequency band appears at 1680 cm$^{-1}$, which shifts to 1640 cm$^{-1}$ with $^{13}CO$ on the Ru–Co catalysts due to the $^{13}CO$ isotope effect. The particular CO bands are also observed at 1680–1684 cm$^{-1}$ on $Ru_3Co/SiO_2$ and $RuCo_2/SiO_2$ catalysts, but negligibly on $[HRu_3(CO)_{11}]^-/SiO_2$ and $Co_4(CO)_{12}/SiO_2$, as well as on the catalysts impregnated from $RuCl_3$ + $CoCl_2$ and $[HRu_3(CO)_{11}]^-$ + $Co_4(CO)_{12}$. A low-frequency band of CO occurred on the conventional Rh–Mn, Rh–Ti, and Rh–Zr/SiO$_2$ catalysts (*8*, *43*), which activate for oxygenate formation in CO hydrogenation, where a large reduction of the CO frequency (1730–1620 cm$^{-1}$) is induced. Shriver *et al.* (*44*) demonstrate that the stoichiometric formation of adducts between metal carbonyls such as $Fe_2(CO)_9$ and

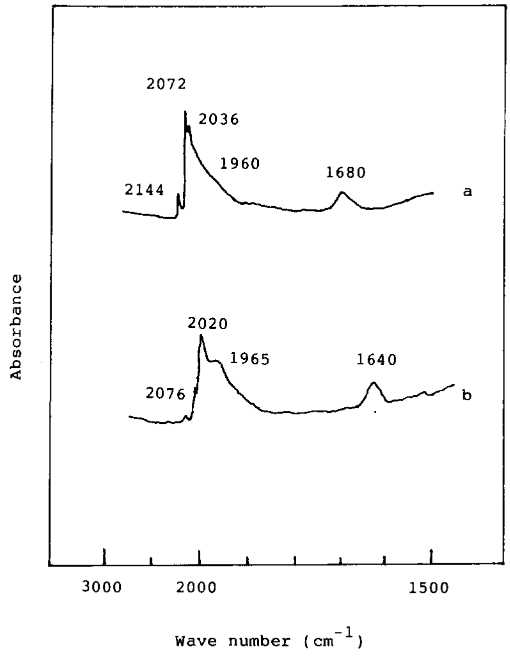

FIG. 8. IR spectra in CO chemisorption at 300–340 K on reduced $Ru_3Co_3C(CO)_{14}$ carbonyl cluster-derived catalyst (reduction for 2 h at 573 K). (a) 100 Torr of CO and (b) 100 Torr of $^{13}CO$.

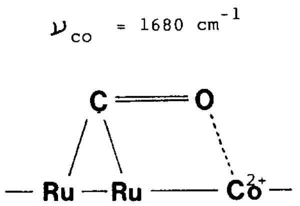

FIG. 9. The proposed structure of two-site CO activation on reduced Ru–Co bimetallic carbonyl cluster-derived catalyst (reduction for 2 h at 573 K).

$Ru_3(CO)_{12}$ and Lewis acids such as $AlCl_3$, $BF_3$, and $\gamma$-$Al_2O_3$ arises from C- and O-bound CO, characteristic of bands at 1740–1520 $cm^{-1}$ and that the rate of methyl migration, i.e., CO insertion, to form the acetyl complex in $Mn(CH_3)(CO)_5$ is greatly enhanced by the adduct formation with $AlBr_3$ and $BF_3$. By comparing the FT-IR data with the structural model of the bimetal cluster-derived catalysts (*3, 45, 46*) it is conceivable that the Ru–Co sites in the catalysts give the two-site CO activation, as in Fig. 9.

### *Chemical Trapping of the 1584 $cm^{-1}$ Species Formed in CO Hydrogenation*

Shown in Fig. 10a are IR spectra recorded after the reaction of CO and $H_2$ with the $H_2$-reduced $RuCo_3/SiO_2$ catalyst for 16 h at 453 K, followed by evacuation to remove the gas phase. In this case, there are many adspecies on the catalyst surface exhibiting 2930, 2860, 2060, 1584, 1465, and 1449 $cm^{-1}$ bands, respectively. Figures 10b–10f show the reaction of surface species with $H_2$ at various temperatures. Exposure of the adspecies to 200 Torr of $H_2$ at room temperature yield no new features in the IR spectra. Increasing the temperature to 458 K leads to a marked decrease of 1584 and 1463 $cm^{-1}$ bands, and the peak positions are shifted to 1560 and 1434 $cm^{-1}$. This suggests that the 1584 $cm^{-1}$ species is much more active than the 1560 $cm^{-1}$ species for reaction with $H_2$ at that temperature. The appearance of the C–H stretching vibration at 3020 $cm^{-1}$ indicates the formation of methane in the gas phase.

Shown in Fig. 11 are analyses of the gas phase recorded after the reaction of adspecies with $H_2$ by using mass spectroscopy. The mass numbers at 13–16 and 29–32 are reasonably assigned to methane and methanol.

The spectra observed after addition of 200 Torr $D_2$ to surface adspecies formed by the reaction of CO + $H_2$ with $RuCo_3/SiO_2$ catalyst for 20 h at 453 K are shown in Fig. 12. At low temperature (room temperature to 423 K) the surface adspecies retain their in-

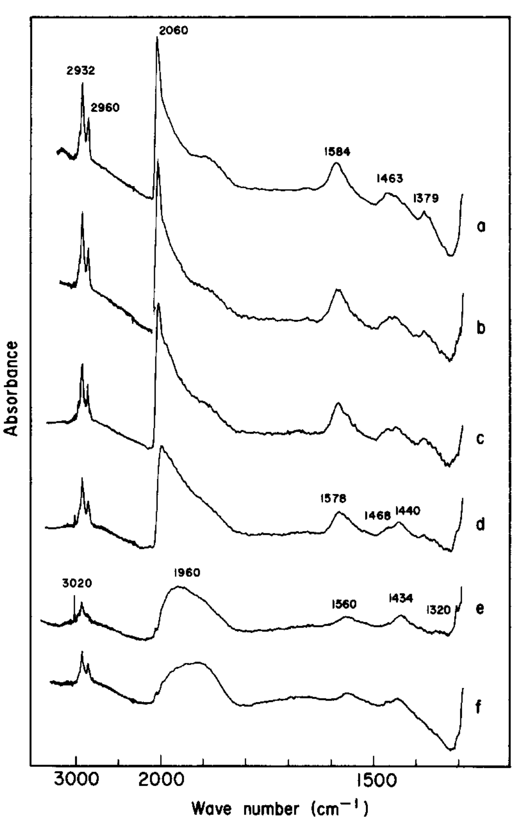

FIG. 10. IR spectra of reaction of $H_2$ with adspecies formed by reaction of syngas with reduced $RuCo_3/SiO_2$ catalyst for 16 h at 453 K (reduction for 2 h at 573 K). (a) After reaction of syngas with sample for 16 h at 453 K, 200 Torr of $H_2$ was introduced into cell system at room temperature; (b) after a, reaction for 20 min at 363 K; (c) after b, reaction for 20 min at 423 K; (d) after c, reaction for 20 min at 443 K; (e) after d, reaction for 20 min at 458 K; and (f) after e, evacuation for 10 min at room temperature.

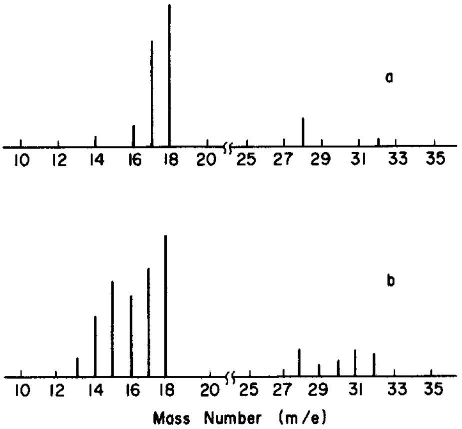

FIG. 11. Mass analysis of products formed by reaction of surface species in $H_2$ + CO reaction with $H_2$ for 30 min at 458 K. (a) Background of mass spectroscopy (vacuum condition $10^{-6}$ Torr), and (b) the gas phase was monitored by mass spectroscopy.

tensities. An increase of temperature to 443 K provides the new bands at 2258 and 2928 $cm^{-1}$ in IR spectra which are assigned to $CHD_3$ (*42*) in the gas phase.

Figure 13 gives the product distribution for mass number after reaction of adspecies with $D_2$, and the two regions at 15–19 and 30–35 for mass number are observed. Mass numbers 15–19 are assigned to $CHD_3$, and the region in 30–35 is assigned to D-labeled methanol. Mass number 35 for D-labeled methanol is proposed to belong to the two possible structures $CHD_2OD$ and $CD_3OH$, formed by the hydrogenation of the surface 1584 $cm^{-1}$ group.

### *X-ray Photoelectron Spectroscopy*

The Co 3*p* and Ru 3*d* spectra of the fresh, reduced, and $RuCo_3$ catalysts were recorded by X-ray photoelectron spectroscopy, as shown in Fig. 14. For the fresh catalyst, Co $3p_{1/2}$ and Co $3p_{3/2}$ spectra exhibit at 796.8 and 780.8 eV, and the Ru $3d_{3/2}$ spectrum gives a very weak shoulder peak at 282.6 eV due to the overlap of C 1*s* and Ru 3*d*, which are consistent with those on the compounds of CoO and ruthenium oxide. After reduction of the catalyst for 3 h at 573 K, a separate peak at 280.4 eV shifted from 282.6 eV is observed. By contrast, the Co 3*p* spectra basically keep their intensity and position. Furthermore, the mixture gases of CO and $H_2$ (40 ml/min, $CO/H_2$ = 1/2) are exposed to the reduced catalyst for 16 h at 453 K, and it is also observed that the peak position and intensity of Co 2*p* and Ru $3d_{3/2}$ are the same as those on the reduced catalyst. These results have demonstrated that, on either the reduced or the used $RuCo_3/SiO_2$ catalyst, the Ru and Co sites

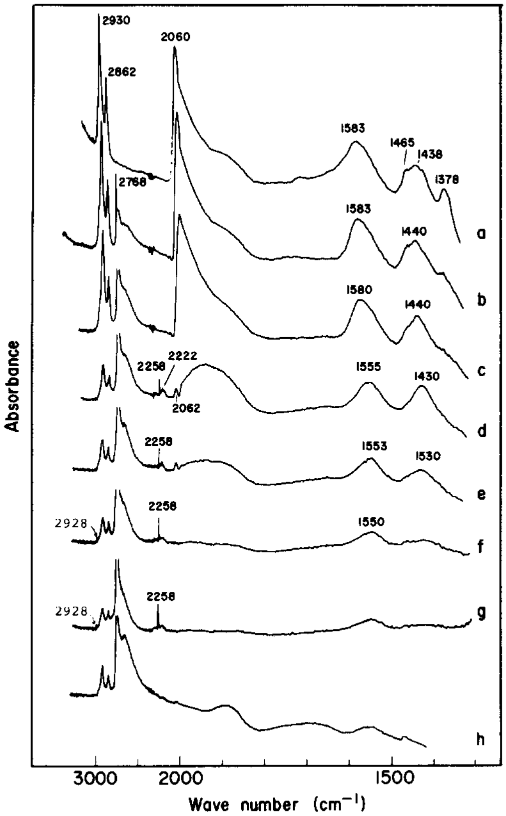

FIG. 12. IR spectra of reaction of $D_2$ with adspecies formed by reaction of syngas with reduced $RuCo_3/SiO_2$ catalyst at 453 K for 16 h (reduction for 2 h at 573 K). (a) 100 Torr $D_2$ for 20 min at room temperature; (b) after a, reaction for 20 min at 373 K; (c) after b, reaction for 20 min at 423 K; (d) after c, reaction for 20 min at 443 K; (e) after d, reaction for 20 min at 473 K; (f) after e, reaction for 20 min at 523 K; (g) after f, reaction for 20 min at 573 K; and (h) after g, evacuation for 20 min at room temperature.

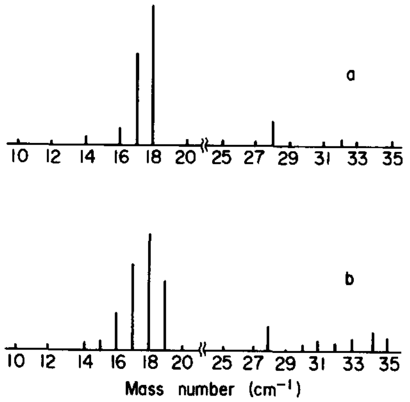

FIG. 13. Mass analysis of products formed by reaction of surface species in CO + $H_2$ reaction with $D_2$ for 30 min at 473 K. (a) Background of mass spectroscopy (vacuum condition $10^{-6}$ Torr), and (b) the gas phase was monitored by mass spectroscopy.

are in chemical states $Ru^0$ and $Co^{2+}$, respectively (*47–50*).

*Effect of Reaction Time and Temperature*

The time dependency of the catalyst was also investigated by FT–IR studies, and the spectra are shown in Fig. 15. Plots of infrared adsorbance of various adspecies versus reaction time during CO hydrogenation provide the curves, given in Fig. 16. At 5 min, a very weak band at 1584 $cm^{-1}$ is observed. With an increase of reaction time from 20 min to 12 h, the bands at 1584 and 1377 $cm^{-1}$ raise intensively, and at 12 h bands that are typical for $CH_3$ and $CH_2$ groups are seen at 2968, 2930, 2856, and 1465 $cm^{-1}$. From the intensity of these bands, we suggest that adsorbed alkyl groups mainly consist of the —$CH_3$ group (*51*). A further increase of reaction time up to 16–20 h adds new features

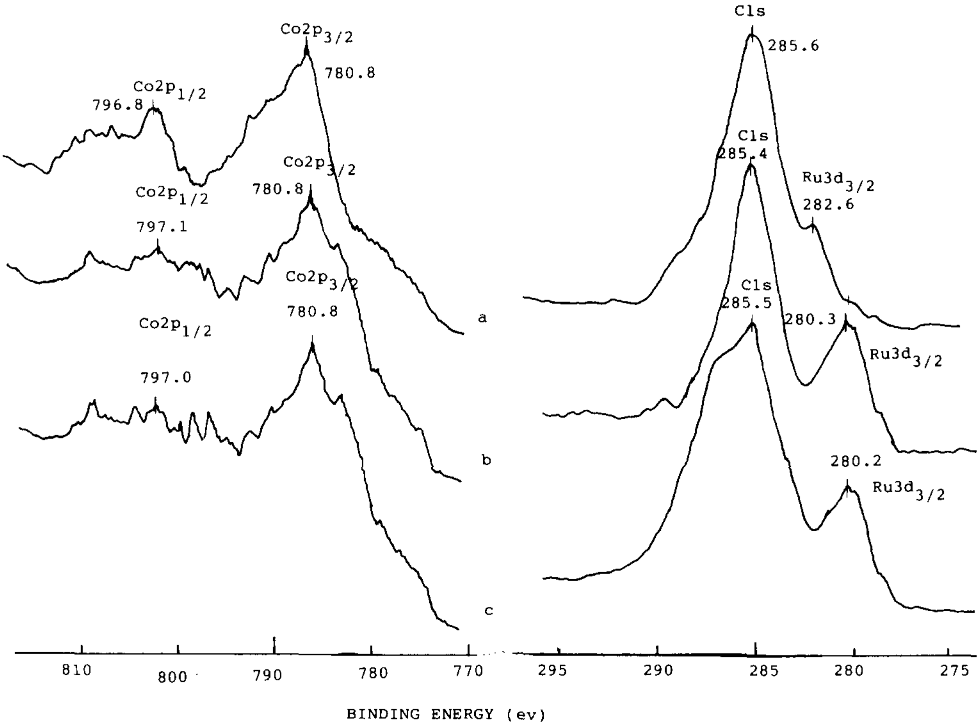

FIG. 14. The XPS spectra of Co 3*p* and Ru 3*d* recorded at (a) fresh $RuCo_3/SiO_2$ catalyst. (b) The $RuCo_3/SiO_2$ was reduced for 2 h at 573 K, and (c) after b, the $RuCo_3/SiO_2$ was exposed to the mixture gases of CO and $H_2$ ($CO/H_2$ = 0.5, 40 ml/min) for 16 h at 453 K.

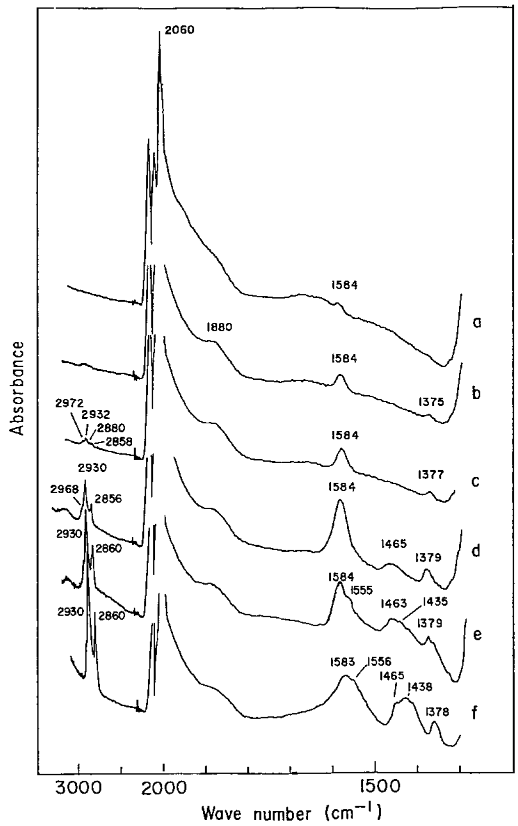

FIG. 15. IR spectra of the RuCo$_3$/SiO$_2$ catalyst after reaction with CO + H$_2$ at 453 K at various times: (a) 5 min, (b) 20 min, (c) 4 h, (d) 12 h, (e) 16 h, and (f) 20 h.

to IR spectra which exhibit at 1555 and 1438 cm$^{-1}$.

Figure 17 shows the spectra of CO + H$_2$ on RuCo$_3$/SiO$_2$ at 503 K. The spectrum of the catalyst after reaction for 20 h in the presence of CO and H$_2$ provides the bands at 1562 and 1448 cm$^{-1}$. Comparing with the 1584 cm$^{-1}$ species formed at 453 K on the same catalyst, it is suggested that the band at 1562 cm$^{-1}$ arises from overlapping of 1555 and 1584 cm$^{-1}$ and that the 1555 cm$^{-1}$ species are predominant in the 1562 cm$^{-1}$ bands.

## DISCUSSION

### *Catalytic Activity and Selectivity in CO Hydrogenation*

The large difference in catalytic performance in CO hydrogenation over the catalysts impregnated from [HRu$_3$(CO)$_{11}$]$^-$, Co$_4$(CO)$_{12}$, and a series of Ru–Co bimetallic carbonyl clusters as well as the impregnation of [HRu$_3$(CO)$_{11}$]$^-$ + Co$_4$(CO)$_{12}$ and RuCl$_3$ + CoCl$_2$ are observed in Table 1. It is interesting to note that the catalysts prepared from a series of Ru–Co bimetallic carbonyl cluster exhibit much higher activity and selectivity for oxygenated products than that on the catalysts prepared from monometallic carbonyl cluster such as [HRu$_3$(CO)$_{11}$]$^-$ or Co$_4$(CO)$_{12}$ and even the coimpregnation of [HRu$_3$(CO)$_{11}$]$^-$ and Co$_4$(CO)$_{12}$. These results demonstrate that the Ru/Co bimetallic sites formed in the Ru–Co bimetallic carbonyl clusters have a strong synergy effect in the formation of oxygenates from CO hydrogenation, possibly owing to the site blocking of Ru ensembles with Co atoms.

### *Relationship between IR bands and Catalytic Performance*

Figures 2 and 3 and Tables 3 and 4 show that there is a good correlation between the yields of C$_1$–C$_5$-oxygenates, including alcohols and aldehydes in CO hydrogenation, and the band intensities at 1584 cm$^{-1}$ on the catalysts from the different Ru–Co carbonyl clusters on SiO$_2$. The particular band around 1584 cm$^{-1}$ could not be observed on Ru$_3$/SiO$_2$, Co$_4$/SiO$_2$, and Ru$_3$ + Co$_4$/SiO$_2$ catalysts under the reaction conditions. On the other hand, we observe no linear relationship between the activity and selectivity for oxygenates in CO hydrogenation and the intensities of 2020 and 1880 cm$^{-1}$ bands formed in CO + H$_2$ reaction. These results demonstrate that the 1584 cm$^{-1}$ species is a very active intermediate in the formation of oxygenates in CO hydrogenation. Moreover, increasing the reaction temperature or/and reaction time leads to the appearance of the 1555 cm$^{-1}$ band, while the 1584 cm$^{-1}$ species decreases considerably, as shown in Figs. 15–17. Therefore, it is suggested that the 1584 cm$^{-1}$ species can be easily converted into the 1555 cm$^{-1}$ species by the

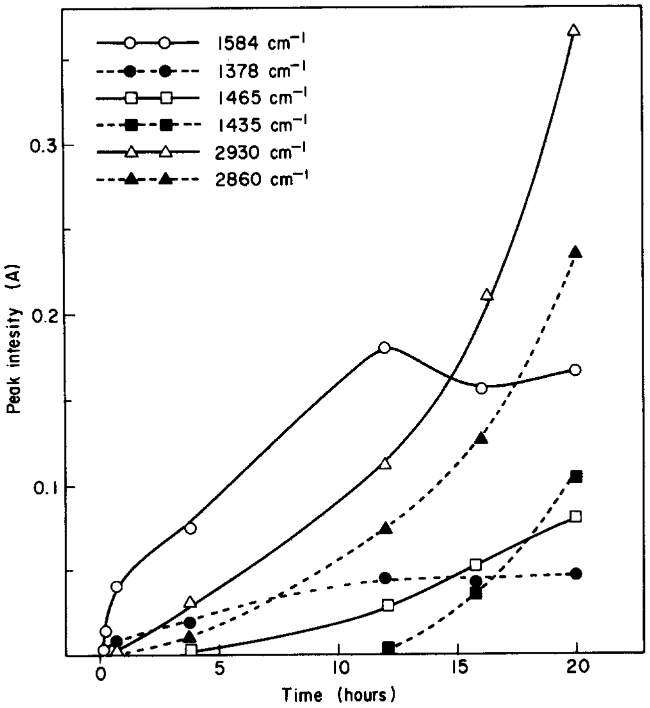

FIG. 16. Plots of IR band intensity versus reaction time on $RuCo_3/SiO_2$ at syngas ($CO/H_2 = 0.5$) and 453 K.

reaction with surface alkyl groups. On the other hand, it has been seen that, by increasing the reaction temperature for CO hydrogenation on $Ru\text{-}Co/SiO_2$ catalysts, the activity and selectivity for higher $C_2$-oxygenates intensively increases, while for methanol the rate considerably decreases, as observed in Table 2. By the comparison of IR spectra and catalytic activity and selectivity for oxygenates in CO hydrogenation, we reasonably believe that it is likely that methanol is directly formed by the hydrogenation of the 1584 $cm^{-1}$ species and that the formation of higher $C_2$-oxygenates results from the hydrogenation of the 1555 $cm^{-1}$ species.

## *Assignment of IR Spectra in CO Hydrogenation*

The IR spectra in CO hydrogenation appear as the bands at 2932, 2860, 2020, 1980, 1880, 1584, 1430, 1465, and 1377 $cm^{-1}$. The bands at 2932–2860 and 1465–1430 $cm^{-1}$ correspond to the C–H stretching and deformation frequency, and the bands at 2080–1980 and 1880 $cm^{-1}$ are easily assigned to linear and bridging CO on Ru surface, which are in good agreement with other researchers (*5, 39, 40, 51*). For the 1584 $cm^{-1}$ band, two possible structures, such as formate and formyl species, are suggested.

Several IR bands in the range from 1600 to 1350 $cm^{-1}$, such as 1590, 1395, and 1375 $cm^{-1}$, are observed for oxide-supported Rh and Ru catalysts, exposed to the mixture of $CO + H_2$ and $CO_2 + H_2$ (*23–29*), and it was suggested that the 1590 and 1375 $cm^{-1}$ bands are attributable to the asymmetric and symmetric OCO stretching vibrations of the formate species and that the 1395 $cm^{-1}$ band was assigned to the C–H deformation mode of the surface formate, respectively. Furthermore, the *in situ* IR spectra showed that

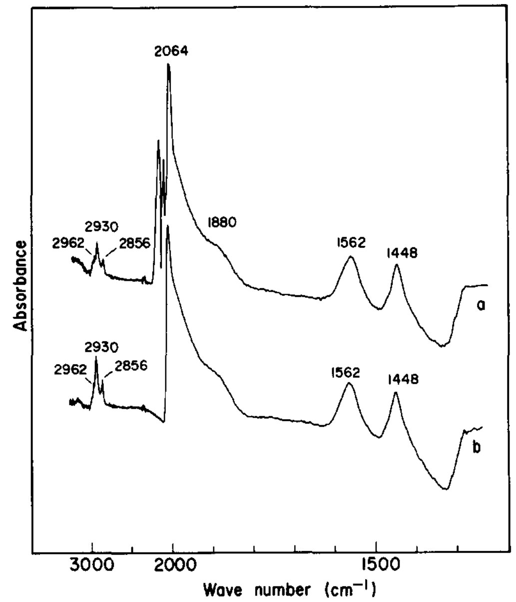

FIG. 17. IR spectra of the reduced RuCo$_3$/SiO$_2$ (reduction for 2 h at 573 K) after reaction with CO + H$_2$ (CO/H$_2$ = 0.5) for 20 h at 503 K (a) before evacuation and (b) after evacuation for 20 min at room temperature.

the adsorption of formic acid on the Rh/Al$_2$O$_3$ (*25*) and the Ru/Al$_2$O$_3$ (*28*) exhibited bands of 1585, 1392, and 1375 cm$^{-1}$, and these adspecies were shifted in the presence of D$_2$ to 1583, 1050, and 1345 cm$^{-1}$, respectively. According to the interpretation, the 1584 and 1377 cm$^{-1}$ bands formed in CO hydrogenation over Ru–Co bimetallic carbonyl cluster-derived catalysts could be assigned to the asymmetric and symmetric OCO stretching frequencies of the formate species, in which one oxygen atom is supported from CO and the other from support, as shown in Fig. 18. With the increase of reaction temperature, the appearance of the 1555 cm$^{-1}$ band could be assigned to the acetate species, which results from the interaction between formate and surface alkyl groups such as $-CH_3$. A similar assignment has been reported by Tamaru *et al.* (*17*) over supported Rh catalysts in CO hydrogenation below atmospheric pressure.

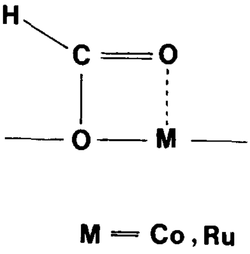

FIG. 18. The proposed model of formate species formed in CO hydrogenation on Ru–Co bimetallic carbonyl cluster-derived catalysts.

On the other hand, we found that the assignment of formate species and isotopic experimental results is apparently not in harmony. It is observed (Figs. 5–7) that the 1584 cm$^{-1}$ bands formed in the mixture gases of CO and H$_2$ at 453 K are shifted to 1575, 1542, and 1539 cm$^{-1}$ in the presence of CO + D$_2$, $^{13}$CO + H$_2$, and $^{13}$CO + D$_2$ at the same reaction temperatures, which are different from the literature (*26*). Therefore, the 1584 cm$^{-1}$ band could not be assigned to formate simply. Notably, if the formyl species is a model of the 1584 cm$^{-1}$ species, it is very interesting to find that the theoretical results (*42*) are the same as the experimental results, summarized in Table 5. Therefore, it is suggested that the 1584 cm$^{-1}$ band is possibly assigned to carbonyl frequency of a surface formyl coordinated to transition metal complexes, where the carbon of formyl species is bounded to Ru metal and the oxygen atom has an interaction with promoter cation Co$^{2+}$, as proposed

TABLE 5

Frequencies of Reaction of CO + H$_2$, $^{13}$CO + H$_2$, CO + D$_2$, and $^{13}$CO + D$_2$ on Ru–Co Bimetallic Carbonyl Cluster-Derived Catalysts

| Syngas | Hydrocarbon bands (cm$^{-1}$) | | Carbonyl bands (cm$^{-1}$) | | |
|---|---|---|---|---|---|
| CO + H$_2$ | 2930 | 2880 | 2064 | 1584 | 1376 |
| CO + D$_2$ | — | — | 2062 | 1575 | — |
| $^{13}$CO + H$_2$ | 2924 | 2848 | 2016 | 1542 | 1345 |
| $^{13}$CO + D$_2$ | 2208 | 2096 | 2104 | 1539 | — |

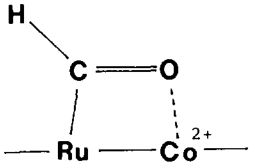

FIG. 19. The proposed model of formyl species formed in CO hydrogenation on Ru–Co bimetallic carbonyl cluster-derived catalysts.

in Fig. 19. In fact, several similar model organometallic compounds exhibit carbonyl frequency of formyl species in the region of 1610–1555 $cm^{-1}$ (*52–57*). Unfortunately, some of the frequencies assigned to characteristic stretching C–H of formyl species lower than 2800 $cm^{-1}$ are not observed, which is possibly due to a small extinction coefficient of C–H vibration. The same phenomenon is found in the model compounds (*56, 57*) and IR studies of CO hydrogenation over $Rh/SiO_2$ catalyst (*58*), where it is only shown as the carbonyl frequency of formyl species and does not have the bands of stretching C–H due to a small extinction coefficient of C–H vibration.

The change of 1377 $cm^{-1}$ species is also observed. The reaction of $^{13}CO + H_2$ and $CO + H_2$ on $Ru_3Co/SiO_2$ indicates that the 1377 $cm^{-1}$ band is not due to the frequency of C–H deformation, and the adspecies also contain a CO group. Davis and Bartean (*59*) have studied the adsorption of aldehydes on Pd(111) surface and suggested that there are two adspecies; one is acetyl at 1565 $cm^{-1}$ ($CH_3C{=}O$) and the other species is characteristic at 1390 $cm^{-1}$ and is represented by $\eta^2$-acetaldehyde. Possibly, the species at 1377 $cm^{-1}$ is assigned to the $\eta^2$-formyl group.

It has been proposed that the $\eta^2$-formyl species could be formed at 453–473 K on palladium/zirconia catalysts (*60*). On the other hand, it has been reported that the formyl species adsorbed on oxide-supported transition metal is unstable. For example, Yates *et al.* found that HCHO is unstable on Rh supported by $Al_2O_3$ and easily converts into the formate species even at 295 K (*61*), which is in contradistinction to the assignment of proposed formyl species formed at 453 K in CO hydrogenation over Ru–Co bimetallic carbonyl cluster-derived catalysts. Generally, the carbonyl stretching frequency of the formyl group should appear near 1700 $cm^{-1}$. Here, in our cases it is proposed that there is an interaction between the oxygen atom of the formyl species and the cobalt ions as the Lewis acidic sites. This interaction would reduce the bond strength between oxygen and carbon atoms in the formyl species and raise the stability of formyl species, producing the 1584 $cm^{-1}$ band in CO hydrogenation over Ru–Co bimetallic carbonyl cluster-derived catalysts.

According to the assignment of formyl species for 1584 $cm^{-1}$, the 1555 and 1438 $cm^{-1}$ species formed in CO hydrogenation at higher temperature could correspond to the carbonyl stretching and C–H deformation of acyl species. Such low carbonyl stretching frequencies of the acyl group have also been observed in $H_2Ru_3(CO)_9CHCH_3CO$ (*62*) and $Mn(CH_3)(CO)_5$ (*44*), reported by Shriver and co-workers.

It has been proposed that C- and O-ended CO characteristic of bands at 1680 $cm^{-1}$ formed on the Ru–Co bimetallic sites of Ru–Co bimetallic carbonyl cluster-derived catalysts under CO atmosphere, as observed in Fig. 8. After reaction with CO and $H_2$, the same catalysts give the bands at 1584 $cm^{-1}$, with the disappearance of the 1680 $cm^{-1}$ band. In contrast, there is no change in the other IR bands such as 2020 and 1880 $cm^{-1}$. Therefore, it is possibly interpreted that the 1584 $cm^{-1}$ species arises from the interaction of the 1680 $cm^{-1}$ species and hydrogen.

The analysis of product distribution in Figs. 10–13 shows that the 1584 $cm^{-1}$ species from $CO + H_2$ is converted with $D_2$ mainly to $CHD_2OD + CHD_3$, which demonstrates that the 1584 $cm^{-1}$ species consists of one H atom and one CO group. This result is consistent with its assignment to a surface formyl species.

By the above discussions, it is suggested that the formyl is more possible than the formate species for the assignment of the 1584 $cm^{-1}$ band formed in CO hydrogenation over Ru–Co bimetallic carbonyl cluster-derived catalysts.

## CONCLUSION

The important conclusions of this study may be summarized as follows:

(1) The activity and selectivity for oxygenates in CO hydrogenation on a series of Ru–Co bimetallic carbonyl cluster-derived catalysts are very high, in contrast to those on $Ru_3/SiO_2$ and $Co_4/SiO_2$ catalysts.

(2) The spectra of the Ru–Co/$SiO_2$ catalysts after the reaction of CO + $H_2$ reveal that the intensity of a band at 1584 $cm^{-1}$ has a good linear relationship with the activity and selectivity for oxygenates in CO hydrogenation and thus it is proposed that the 1584 $cm^{-1}$ species is an important intermediate in production of oxygenates.

(3) The increase of reaction time and temperature in CO hydrogenation over Ru–Co/$SiO_2$ catalysts leads to the appearance of a new band at 1555 $cm^{-1}$, which arises from the reaction of the 1584 $cm^{-1}$ species with the surface-adsorbed alkyl group. From a comparison of the product distribution at various temperatures, it is suggested that the 1584 and 1555 $cm^{-1}$ species are intermediates for methanol and higher $C_2$-oxygenates, respectively.

(4) The adsorption of CO on reduced Ru–Co/$SiO_2$ catalysts prepared from Ru–Co bimetallic carbonyl clusters exhibits a band at 1680 $cm^{-1}$ shifting to 1640 $cm^{-1}$ with $^{13}CO$, which is assigned to the C- and O-ended chemisorbed on Ru–Co/$SiO_2$ catalysts.

(5) The 1584 $cm^{-1}$ species show two possible structures, formate and formyl. The reaction of D- and $^{13}C$-labeled CO and $H_2$ leads to the assignment of the 1584 $cm^{-1}$ band to the formyl group, the chemical trapping of 1584 $cm^{-1}$ shows that the hydrogenation of the 1584 $cm^{-1}$ species produces $CH_4$ and $CH_3OH$, and the reaction of the 1584 $cm^{-1}$ group with $D_2$ results in the formation of $CHD_3$ and $CHD_2OD$, in good agreement with the formyl model.

## ACKNOWLEDGMENTS

This work was supported by the JSPS and NSF Japan–U.S. Cooperative Science Program (1989–1990) and the National Natural Science Foundation of China. We greatly thank Professor D. F. Shriver and W. Henderson for the synthesis of $Ru_3Co_3C(CO)_{14}$ cluster and for valuable suggestions.

## REFERENCES

1. Ichikawa, M., *in* "Tailored Metal Catalysts," (Y. Iwasawa and D. Reidel, Eds.). Dordrecht, 1985.
2. Gates, B. C., Guczi, L., and Knozinger, H., Eds., *in* "Metal Cluster in Catalysis." Elsevier, Amsterdam, 1986.
3. Ichikawa, M., *Polyhedron* **7,** 2351 (1988).
4. Choplin, A., Huang, L., Theolier, A., Gallezot, P., Basset, J. M., Siriwardane, U., Shore, S. G., and Mathien, R., *J. Am.Chem. Soc.* **108,** 4224 (1986).
5. Xiao, F.-S., Fukuoka, A., Henderson, W., Shriver, D. F., and Ichikawa, M., *Catal. Lett.* 6, 361 (1990).
6. Ichikawa, M., Fukushima, T., and Shikakura, K., *in* "Proceedings, 8th International Congress on Catalysis, Berlin, 1984," Vol. 2, p. 69. Dechema, Frankfurt-am-Main, 1984.
7. Fukushima, T., Arakawa, K., and Ichikawa, M., *J. Phys. Chem.* **89,** 4440 (1985).
8. Fukushima, T., Araki, K., and Ichikawa, M., *J. Chem. Soc. Chem. Commun.,* 148 (1986).
9. Fukuoka, A., Ichikawa, M., Hriljac, J. A., and Shriver, D. F., *Inorg. Chem.* **26,** 3643 (1987).
10. Fukuoka, A., Rao, L-F., and Ichikawa, M., *Catal. Today* **6,** 55 (1989).
11. Ichikawa, M., Fukuoka, A., and Kimura, T., *in* "Proceedings, 9th International Congress on Catalysis, Calgary, 1988" (M. J. Phillips and M. Ternan, Eds.), Vol. 2, p. 259. Chem. Institute of Canada, Ottawa, 1988.
12. Wentrcek, P. R., Wood, B. J., and Wise, H., *J. Catal.* **43,** 363 (1976).
13. Araki, M., and Ponec, V., *J. Catal.* **44,** 439 (1976).
14. Sachtler, J. W. A., Kool, J. M., and Ponec, V., *J. Catal.* **56,** 284 (1979).
15. Biloen, P., Helle, J. N., and Sachtler, W. M. H., *J. Catal.* **58,** 95 (1979).
16. Cant, N. W., and Bell, A. T., *J. Catal.* **73,** 257 (1982).
17. Orita, H., Narita, S., and Tamaru, K., *J. Chem. Soc. Chem. Commun.,* 150 (1984).
18. Channette, P., *et al., in* "Proceedings 9th International Congress on Catalysis, Calgary, 1988" (M. J. Phillips and M. Ternan, Eds.), Vol. 2. Chem. Institute of Canada, Ottawa, 1988.

*19.* Fukushima, T., Arakawa, H., and Ichikawa, M., *J. Chem. Soc. Chem. Commun.*, 730 (1985).
*20.* Ichikawa, M., and Fukushima, T., *J. Phys.Chem.* **89,** 1564 (1985).
*21.* Kikuzono, Y., Kagami, S., Naito, S., Onishi, T., and Tamaru, K., *Chem. Lett.*, 1249 (1981); *Faraday Discuss. Chem. Soc.* **72,** 135 (1981).
*22.* Takeuchi, A., and Katzer, J. R., *J. Phys. Chem.* **86,** 2438 (1982).
*23.* Solymosi, F., Erdohelyi, A., and Kocsis, M., *J. Catal.***75,** 219 (1982).
*24.* Solymosi, F., Erdohelyi, A., and Bansagi, T., *J. Catal.* **68,** 371 (1981).
*25.* Solymosi, F., Erdohelyi, A., and Kocsis, M., *J. Catal.* **65,** 428 (1980).
*26.* Solymosi, F., Erdohelyi, A., and Bansagi, T., *J. Chem. Soc. Faraday Trans. 1* **77,** 2645 (1981).
*27.* Amenomiya, Y., *Appl. Spectrosc.* **32,** 484 (1978).
*28.* Datta Betta, R. A., and Shelef, M., *J. Catal.* **48,** 48 (1977).
*29.* Amenomiya, Y., *J. Catal.* **57,** 64 (1979).
*30.* Xiao, F.-S., Ichikawa, M., and Guo, X.-X., *Bull. Sci.* **36,** 960 (1991). [In Chinese]
*31.* Ichikawa, M., Xiao, F.-S., Magpanty, C. G., Fukuoka, A., Henderson, W., and Shriver, D. F., *in* "Proceedings, Natural Gas Conversion Synthesis Symposium, Oslo, Aug. 12–17, 1990."
*32.* Ichikawa, M., Xiao, F.-S., Magpanty, C. G., Fukuoka, A., Henderson, W., and Shriver, D. F., *in* "Natural Gas Conversion" (A. Holmen, K.-J. Jens, and S. K. Kolboe, Eds.). Elsevier, Amsterdam, 1991.
*33.* Xiao, F.-S., Ichikawa, M., Fukuoka, A., Henderson, W., and Shriver, D. F., *in* "Proceedings, 7th Symposium on the Relation between Homogeneous and Heterogeneous Catalysis, Tokyo, May 17–21, 1992."
*34.* Xiao, F.-S., Ichikawa, M., Fukuoka, A., Henderson, W., and Shriver, D. F., unpublished results.
*35.* Johnson, B. F. G., Lewis, J., Raithby, P. R., and Suss, G., *J. Chem. Soc. Dalton Trans.*, 1356 (1976).
*36.* Steinhart, P. C., Glandfelter, W. L., Hanley, A. D., Fox, J. R., and Geoffroy, G. L., *Inorg. Chem.* **19,** 332 (1980).
*37.* Hidai, M., Fukuoka, A., Koyasu, Y., and Uchida, Y., *J. Chem. Soc. Chem. Commun.*, 516 (1984).
*38.* Henderson, W., and Shriver, D. F., unpublished results.
*39.* Brown, M. F., and Gonzalez, R. D., *J. Phys. Chem.* **80,** 1731 (1976); Kuznetsov. V. L., Bell, A. T., and Yermakov, Y. I., *J. Catal.* **65,** 374 (1980).
*40.* Luchesi, P. J., Cater, J. L., and Yates, D. J. C., *J. Phys. Chem.* **66,** 1451 (1962).
*41.* Xiao, F-S. and Ichikawa, M., unpublished results.
*42.* Pinchas, S., and Laulicht, I., *in* "Infrared Spectra of Labeled Compounds." Academic Press, New York, 1971.
*43.* Sachtler, W. M. H., and Ichikawa, M., *J. Phys. Chem.* **90,** 1752 (1990).
*44.* Horwitz, C. P., and Shriver, D. F., *Adv. Organomett.* **23,** 219 (1984).
*45.* Kimura, T., Fukuoka, A., Fumagalli, A., and Ichikawa, M., *Catal. Lett.* **2,** 227 (1989).
*46.* Ichikawa, M., Fukuoka, A., and Kimura, T., *in* "Proceedings, 9th International Congress on Catalysis, Calgary, 1988" (M. J. Phillips and M. Ternan, Eds.), Vol. 2, p. 259. Chem. Institute of Canada, Ottawa, 1988.
*47.* Kim, K. S., *Phys. Rev. B* **11,** 2177 (1975).
*48.* Folksson, B., *Acta. Chem. Scand.* **27,** 287 (1973).
*49.* Chln, R. L., and Hercules, D., *J. Phys. Chem.* **86,** 360 (1982).
*50.* Helms, C. R., and Sinfelt, J. H., *Surf. Sci.* **72,** 229 (1978).
*51.* Little, L. H., *in* "Infrared Spectra of Adsorbed Species." Academic Press, New York, 1966.
*52.* Collins, T. J., and Roper, W. R., *J. Chem. Soc. Chem. Commun.*, 1044 (1976).
*53.* Gladyz, J. A., and Selover, J. C., *Tetrahedron Lett.* **4,** 319 (1978).
*54.* Pruett, R. L., Schoening, R. C., Vidal, L. J., and Fiato, R. A., *J. Organomet. Chem. C* **57,** 182 (1979).
*55.* Collman, J. P., and Winter, S. R., *J. Am. Chem. Soc.* **95,** 4089 (1973).
*56.* Casey, C. P., and Neumann, S. M., *J. Am. Chem. Soc.* **98,** 5395 (1976).
*57.* Wong, W. K., Tam, W., Srrovese, C. E., and Gladysez, J. A., *J. Chem. Soc. Chem. Commun.*, 530 (1979).
*58.* Orita, H., Narita, S., and Tamuru, K., *J. Catal.* **90,** 183 (1984).
*59.* Davis, J. L., and Bartean, M. A., *J. Am. Chem. Soc.* **111,** 1782 (1989).
*60.* Schild, C., Wokaun, A., and Baiker, A., *J. Mol. Catal.* **63,** 223 (1990).
*61.* Yates, J. T., Worley, S. D., Duncan, T. M., and Vaughan, R. W., *J. Chem. Phys.* **70,** 1225 (1979).
*62.* Sailor, M. J., Brock, C. P., and Shriver, D. F., *J. Am. Chem. Soc.* **109,** 6015 (1987).